Fibers and Polymers 2020, Vol.21, No.4, 724-732
DOI 10.1007/s12221-020-8666-9

ISSN 1229-9197 (print version)
ISSN 1875-0052 (electronic version)

Characterization of Fiber Extracted from *Agave americana* after Burial in Soil

Afef Mansouri[1,2]*, Jalel Ben Nasr[1], Mohamed Ben Amar[1], and Foued Elhalouani[1]

[1]*Electromechanical Systems Laboratory LASEM, National Engineering School of Sfax, University of Sfax, Sfax 3038, Tunisia*
[2]*Faculty of Sciences of Gabes, University of Gabes, Gabes 6072, Tunisia*

(Received July 25, 2018; Revised September 7, 2019; Accepted September 11, 2019)

Abstract: This work presents the characterization of the physico-chemical, thermal, and morphological properties of the Buried Fiber (BF) extracted from *Agave americana L* plant leaves that were submitted to burial in soil. The results showed the main components of these BF are cellulose (63.12 %), hemicelluloses (17 %) and lignin (5.02 %). In addition, their crystallinity index is (53 %) with crystalline size of 2.87 nm. Finally, their thermo gravimetric analysis indicates that they are thermally stable until 215 °C. These results suggest that these BF can be used as suitable reinforcement fibers for bio composites.

Keywords: *Agave americana L* fibers, Fibers extraction, Buried in soil, Characterization, SEM

Introduction

Lignocellulosic fibers are available in large quantity in the world and offer many advantages such as biodegradability, recyclability, lower cost, low density, non-toxicity and reduced environmental impact [1]. Additional benefits include energy savings, renewability of the resource, good thermal and mechanical properties [2]. The main components of fibers are cellulose, hemicelluloses and lignin. They contain a major rate of cellulose, which enhances the mechanical properties of fibers. The main types of ligno-cellulosic fibers are classified according to their location in the plant, for example: bast fibers (jute, kenaf, ramie, hemp, and flax), leaf fibers (agave, abaca, sisal, and pineapples), seed fibers (cotton, coir, and kapok), fruit fibers (fiber coconut), grass and reed fiber (wheat, rice, and maize), and other types (wood) [3].

Lignocellulosic fibers have been investigated by many authors. Common names of *Agave americana* are *American aloe* or *maguey*. Agave belongs to the monocotyledonous family called Agaveceae [4]. *Agave americana* flourishes in South Africa as well as the Mediterranean area [5]. In Tunisia, this plant is the most abundant variety of agave. The color of the fiber varies from milky white to golden yellow.

Many industrial sectors extracted fibers from plants and implemented them in various applications. For example, they used them for the reinforcement of composite materials, such as *Agave americana L* [6], Bamboo [7], Sisal [8] and Alfa [9]. In particular, *Agave americana L*. was used in textiles [5], and in paper pulp [10]. This variety was characterized as a voluminous plant and rigid due to the existence of lignin on its surface [4,11].

Agave fibers were extracted through the mechanical [12], chemical, biological [13] and water retting methods [14,15]. Unfortunately, all these methods had shortcomings. Indeed, both water retting and the biological methods were considered costly in terms of water consumption and labor requirement [16]. Additionally, the water retting process was considered environmentally problematic at an industrial scale due to the large volume of polluted water [17] and unpleasant smell produced by the anaerobic fermentation [18]. For these reasons, Bezazi *et al*. [19] proposed the BF extraction through burying the *Agave americana L* leaves in the soil. However, these scholars focused only on the mechanical properties. Hence, the main objective of this work was to further investigate this process and attempt to characterize of the physico-chemical, thermal, and morphological properties of the Buried Fiber (BF) extracted from *Agave americana L* plant leaves. It is expected to confirm the primacy of this method as an environmentally friendly and cost effective approach the better understand and valorize the *Agave americana L* as a source of valuable fibers that can have many industrial applications.

Experimental

Materials

The *Agave americana L* plant used in this study was obtained from the Sousse region, known as the Sahel region (Tunisia). The soil used to bury the leaves of this plant was that available in the garden of the National Engineering School of Sfax, Tunisia.

Preparation of the Plant

After harvest, the Agave leaves were washed in water. The thorns were removed. Then the leaves were buried 30 cm deep in the soil, as the 20-30 cm soil depth range is the most biologically active, with abundance of soil microbial communities [20].

The principle consists in burying the Agave leaves under a layer of soil. This method rests on the activity of microorganisms in the soil, the combined action of sun and rain favoring the development of microorganisms capable of decomposing the binding natural matrix between the fibers

*Corresponding author: afeffmansouri@gmail.com

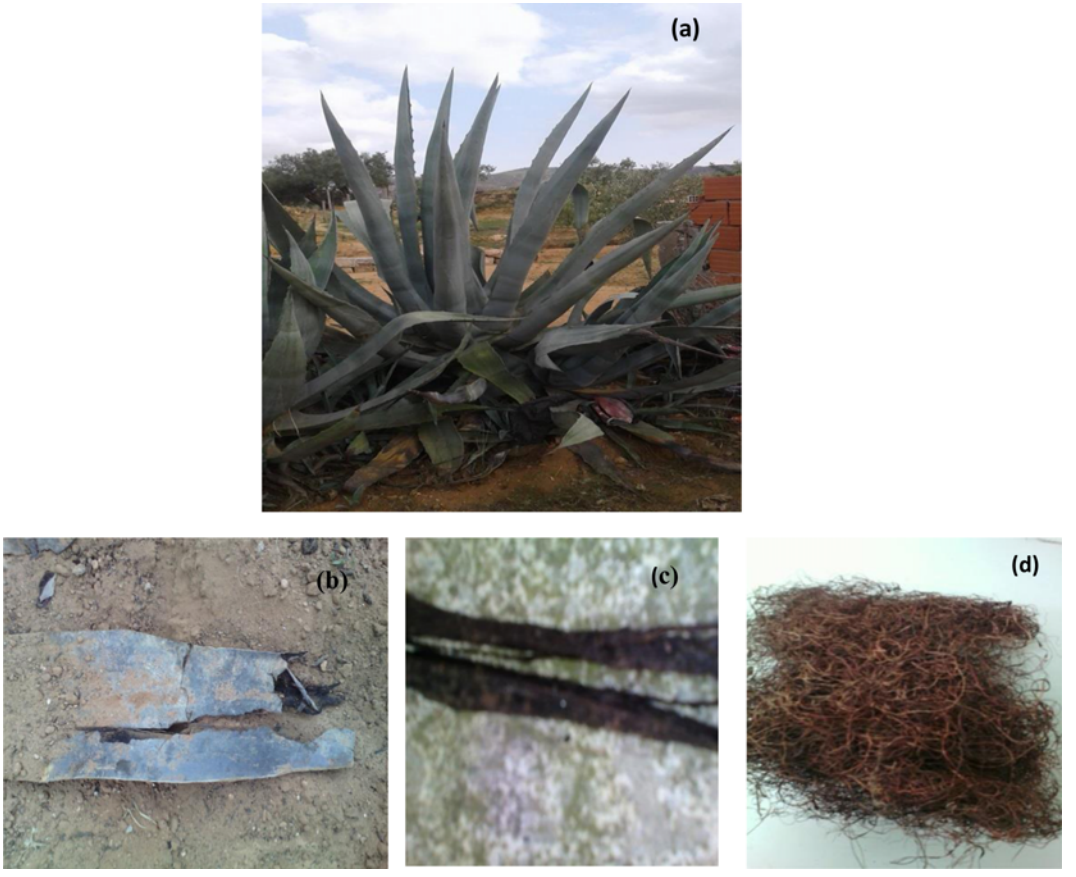

Figure 1. (a) *Agave americana L* plant, (b) leaves of *Agave americana L* before burial, (c) leaves after burial (decomposition of a natural matrix), and (d) the obtained fibers.

[21]. This operation lasted 45 days from 13 September to 28 October which corresponds to the autumn in Tunisia. During the burying period, the weather temperature was recorded in the morning and in the evening. It ranged between 18 and 33 °C. this procedure was conducted because the weather conditions were said to affect the enzymatic activity in general ways [22]. Once this period of burial was over, the fibers were separated manually. The fibers obtained (FB: buried fiber) were washed 4 to 5 times in distilled water to remove any remaining unwanted materials from the fiber surface. Finally, fiber bundles were dried in the oven at 70 °C during 24 hours to remove moisture as is shown in Figure 1.

Chemical Analyses of Fiber

The determination of the basic chemical composition was conducted following ASTM standard protocols. Samples were first submitted to reflux extraction with ethanol/toluene (ASTM D1107-96) [23] and water (ASTM D1110-84) [24]. The chemical contents were determined using the following methods: lignin (ASTM D1106-96) [25], holo-cellulose (ASTM D1104-56) [26], alpha-cellulose (ASTM D1103-60) [27] and ash (ASTM D1102-84) [28].

The vegetal organic matter was calculated by the difference: MO=100−% ash [29].

The nitrogen content was determined according to the Kjeldah method [30].

Chemical Analyses of Soil

The chemical elements of soil were analyzed by atomic absorption spectrometry.

The carbon dioxide content was reckoned by the addition of hydrochloric acid to the calcium carbonate, and measured by a volumetric method with a Bernard calcimeter.

Organic carbon content was determined with method developed by Walkley and Black [31], and converted to Soil organic matter content by a factor of 1.724 [32].

Fourier Transform-infrared (FTIR) Spectrometry

A Fourier Transform-infrared (ATR-FTIR) spectroscopy study of fibers was carried out using a Perkin-Elmer instrument at room temperature. This instrument is driven by computer software (Perkin Elmer Spectrum) with spectral resolution of 4 cm^{-1} and over wave number range of 4000 cm^{-1}-400 cm^{-1}.

X-ray Diffraction (XRD)

The powder of BF was subjected to the X-ray diffraction (XRD) analysis using a Xpert-Pro diffractometer with diffracted intensity of Cu Kα radiation wavelength of 0.154 nm. The operating range was maintained between 10 ^{o} and 60 ^{o} (2θ).

The XRD, used to determine the crystallinity index (I_{Cr}), was computed by Segal method by equation (1) using the height of the 002 peak (I_{002}, 2θ=22.7 ^{o}) and the minimum between the 002 and 110 peaks (I_{AM}, 2θ=18 ^{o}). I_{002} represents both crystalline and amorphous material while I_{AM} represents amorphous material only [33].

$$I_{cr} = \left[\left(\frac{I_{002} - I_{AM}}{I_{002}}\right) \times 100\right] \quad (1)$$

Crystallite size (L) was computed via Scherer's formula

$$L = \frac{K\lambda}{\beta \cos\theta} \quad (2)$$

where L is the crystallite size perpendicular to the plane; K= 0.89, is the Sharer's constant, λ=0.1541 nm is the wavelength of the radiation, β is the peak's full-width half-maximum (FWHM) in radians and θ is the Bragg angle.

The equation that classifies the cellulose Iα and Iβ type is [34]:

$$Z = 1693d_1 - 902d_2 - 549 \quad (3)$$

where

d_1 is the d-spacing of (1-10) peak

d_2 is the d-spacing of (110) peak

Thermal Analysis

The thermal stability of buried fiber (BF) was performed using a Perkin Elmer Pyris 6 TGA analyzer in a nitrogen atmosphere. The sample was heated from room temperature to 800 ^{o}C at a rate of 10 ^{o}C/min with a nitrogen gas flow rate of 40 m*l*/min. A derivative thermo-gravimetric (DTG) curve was calculated from the TGA data.

Scanning Electron Microscope

Observation of the microstructure of the fibers was performed by scanning electron microscope (Jeol, JSM-540).

Results and Discussion

Chemical Characterization of the BF Obtained Through Leaf Burial in the Soil

Table 1 shows the chemical composition of the *Agave americana L* leaf fibers. Firstly, it is worth observing that the adoption of the leaf burying in soil method yielded a relatively high content of cellulose (63.12 %). Compared to the cellulose content obtained from the manual extraction and the retting in seawater methods, our method proved more efficient. Indeed, the former methods yielded 59 % and 62.3 % cellulose content respectively [35]. In addition, although the retting in distilled water method yielded 65.2 %, it was criticized for being more costly and environment damaging [35]. The search for high cellulose content was justified by its role in enhancing the tensile strength and young's modulus of fibers [36]. The second important result is related to the lignin content in the obtained fibers. The *Agave americana L* leaves contained 5.02 % of this substance after their burial in the soil. This content was much higher than the 2.1 % lignin content of the untreated *Agave* characterized by [35]. More importantly, it exceeded the lignin content obtained from *Agave americana L* treated with NaOH concentrations of 1 and 10 %. Indeed, in both cases, the lignin content was 2.61 % and 2.34 %, respectively [37]. The remarkable presence of lignin can be explained by the fact that it is the most resistant fraction of the plant and the last compound to be decomposed by soil microorganisms. Lignin presents many advantages because it can act as a shield against biological attack on fibers. In addition, it plays

Table 1. Characterization of the fibers after burial in the soil

Name of plant	Method of extraction	Cellulose (%)	Hemicellulose (%)	Lignin (%)	Pectin (%)	Ash (%)	Reference
Buried fiber (BF)	Burial in soil	63.12	17	5.02	6.92	7.43	Present work
Agave Americana	Raw	59	38.4	2.5			[35]
Agave Americana	Treated with distilled water	65.2	32.1	2.7			[35]
Agave americana	Treated with seawater	62.3	35.6	2.1			[35]
Agave Americana	Treated with 1 % NaOH	69.89	27.49	2.61			[37]
Agave Americana	Treated with 10 % NaOH	70.35	27.29	2.34			[37]
Alfa	Treated with saltwater	59.84	24.3	12.66			[45]
Posidonia oceanica	Mechanical	44.2	18.3	29.3	6.72	12.03	[46]
Prosopis juliflorabark	Treated with water	61.65	16.14	17.11		5.2	[43]
Sponge-gourd	Raw	59.42	16.50	16.36			[47]
Cordia dichotoma	Treated with water	59.7	23.6	14.7			[48]

an important role in protecting the hemicellulose and cellulose [36,38,39]. Consequently, it reinforces to the fiber structure, property, and morphology [40]. The third interesting finding of this work was the decrease in the hemicelluloses content to 17 % compared to other extraction methods. This content of hemicelluloses in *Agave americana L.* leaves treated by sea water and alkaline treatment was 35.6 % and 27.49 %, respectively [35,37]. This reduction was explained by the breakage and disruption of hydrogen bond [41]. Indeed, hemicelluloses was considered to be the first fraction which decomposes in the soil because it is used by microorganisms as their carbon and energy source [38,42]. Its decrease represents another advantage to the quality of the fibers. Indeed, the lesser hemicelluloses there is, the stronger the fiber becomes. Its high presence leads to degradation and disintegration of micro fibers [43]. The fourth finding is related to the ash content in the fibers. As can be seen in Table 1, the 7.43 % ash content found in the BF from the *Agave americana L* leaves after burying them in the soil is higher than the 5.28 % of ash observed by Yang [44]. Ash is known for its large variety of inorganic minerals such as Ca, Mg, Fe, and Na, along with extra trace metals exhibited in Table 3. The high content of ash was explained by Mushtaq *et al*., Khalil *et al.* and Kögel-Knabner [49-51] as a result of the fast decomposition of organic matter in the soil. Indeed, microorganisms use organic compound as a source of nutrition. Hence, the longer the leaves of *Agave americana L* remain buried in the soil, the lesser they keep their organic matter and the higher their content in ash becomes.

Characterization of the Burial Soil

The chemical composition of the burial soil is shown in Table 2. Firstly, it was observed that the organic matter in the burial soil rose from the original 1.27 % rate to a 1.94 % rate after burial. This increase in organic matter was explained by Kögel-Knabner [51] as a consequence of the plant release of organic matter such as carbon and nitrogen into the burial soil. Specifically, organic carbon in the burial soil rose from an original rate of 0.74 % to a 1.13 % rate after burial. Similarly, nitrogen rate increased from 0.05 % to 0.10 % in the burial soil. This increase was rightly explained by the translocation of the plant organic matter to the soil. Hence the burial method seems to have a positive effect on the soil since it contributes to increase carbon which is a source of energy for the microorganisms in the soil [52,53]. Equally, Nitrogen is an essential macronutrient of the plant. It promotes growth as well as the increase of the yield of plant biomass. Therefore, it optimizes fiber quality [50]. The nitrogen contents of fibers are 0.38 %.

Secondly, the relative carbon (C) and nitrogen (N) contents are expressed by their ratio (C/N) of soil. Indeed, this ratio 12.81 and 11.15 % before and after burial, respectively, shows a decrease which is due to an increase in biological activity.

Thirdly, there was an observed decrease in phosphorus P_2O_5 from 0.11 % before the burial of *Agave americana L* leaves to 0.03 % after burial. This decrease was explained by Halder and Chakrabartty [54] as an expression of the solubilization of the phosphorus by the microorganism in soil. Fourthly, there was an observation of an increase of calcium content by 15.8 % in the soil after the burial of *Agave americana L* leaves. As was rightly reported by Ledin *et al.* [55], this was caused by the important role of micro-organisms in the metal mobility in soil resulting in the increase of calcium content.Finally, there was a clear rise of the CO_2 rate in the soil after the burial of *Agave americana L* leaves. Indeed, it is increased from 3.58 % before the burial to 4.43 % after the burial. Sadowsky and Schortemeyer [56] considered the increase in CO_2 as a proof of the increase of the microbial activity in the soil. All these observations seem to converge to prove that the burial of *Agave americana L* leaves in soil may serve a two-fold objective. Simultaneously with the improvement of the extracted fibers, it enhances the quality of the fibers and exploits the activity of the micro-organisms. Hence, besides the efficiency of this method, it is cost effective and environmentally friendly.

Table 2. Characterization of the burial soil

	Carbon (%)	Organic matter (%)	N (%)	C/N	CO_2 (%)	P_2O_5 (%)	CaO (%)	MgO (%)	Fe_2O_3 (%)	Al_2O_3 (%)	Na_2O (%)	K_2O (%)	SiO_2
Before burial of leaves in soil	0.74	1.27	0.05	12.81	3.58	0.11	2.39	0.47	0.78	0.39	0.07	1.22	62.98
After burial of leaves in soil	1.13	1.94	0.10	11.15	4.43	0.03	2.77	0.60	0.79	0.38	0.06	1.22	58.76

Table 3. Chemical composition contents of BF

Element	Organic matter	N	CaO	MgO	Fe_2O_3	Al_2O_3	Na_2O	K_2O
Percentage (%)	92.57	0.38	1.37	0.59	0.03	0.01	0.02	0.01

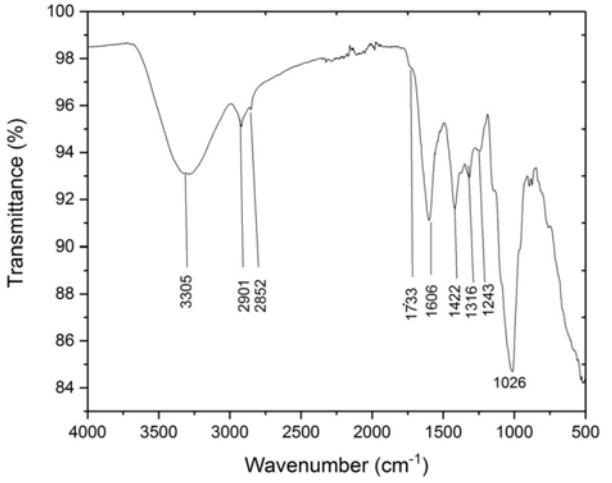

Figure 2. FTIR spectrum of a BF.

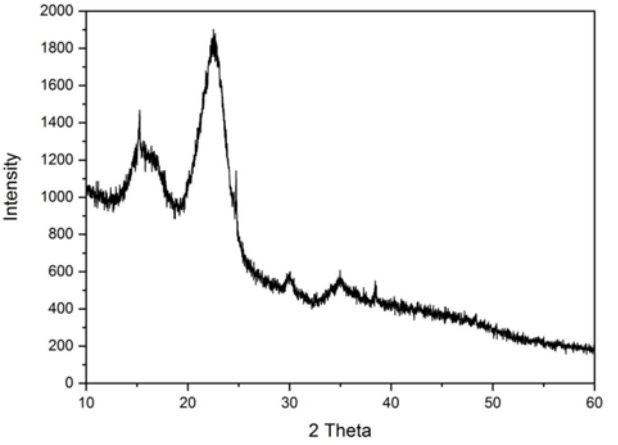

Figure 3. X-ray spectrum of a BF.

Analysis of the FTIR Spectrometry of a BF

The BF are analyzed using FTIR vibration spectrum to evaluate the absorption bands of different functional chemical groups such as cellulose, hemicelluloses and lignin. As shown in Figure 2, a broad absorption band in the area 3600-3100 cm^{-1} corresponds to the O-H stretching vibrations characteristic of hydroxyl groups bonded to hydrogen. In line with Sathishkumar *et al.*, these can be attributed to cellulose Iβ [57]. The broad peak is centered at 3305 cm^{-1}. In light of this observation, the BF obtained after burial of the *Agave americana L* leaves in the soil would certainly belong to the cellulose I structure. This finding will be crosschecked by the X-ray analysis below. However the two bands 2901 and 2852 cm^{-1}, assigned to CH and CH_2, would be components of cellulose and hemicelluloses as was interpreted by in a previous work by Sathishkumar *et al*. [57]. The small sharper peaks at 2089 to 2323 cm^{-1} would correspond to the asymmetrical vibrations confirming the presence of wax or wax list gist. A similar peak value was reported for *Prosopis juliflora* fibers at 2355 cm^{-1} [58], *Calotropis gigantean* fibers at 2133 cm^{-1} [59] and *Coccinia grandis* fibers 2345 cm^{-1} [60]. The small protrusion at 1735 cm^{-1} can be attributed to the stretching vibration from the carbonyl C=O of linkage of carboxylic acid in lignin or ester group in hemicelluloses group as was reported by Reddy *et al.* [61] in their work on native African Napier grass [61]. The intense peak to 1606 cm^{-1} can be associated with the aromatic compound found in the structure of lignin as was interpreted by Porras *et al*. [62]. The bands at 1422 and at 1316 cm^{-1} can be interpreted as indicators of crystalline cellulose while the band at 896 cm^{-1} can be due to amorphous cellulose in line with an interpretation by Pereira *et al.* [63]. These characteristic peaks prove the cristallinity of these BF. This will be further confirmed by the analysis of the XRD, below. In total agreement with [64], the peak localized at 1243 cm^{-1} would correspond to the -COO vibration of acetyl groups in hemicelluloses. However, the peak at 1160 cm^{-1} would indicate the presence of COC anti-symmetric stretching in cellulose and hemicelluloses as was revealed by [65]. The strong absorption peak at 1026 cm^{-1} can be attributed to CO and OH stretching vibrations because of the polysaccharide in cellulose as was explained in a previous work by [66]. In line with [66], The absorption peak at 890 cm^{-1} would represent the typical structure of cellulose showing C-O-C stretching vibration of β, 1,4-glycosidic linkages triggered by cellulose.

The two minimal leveling outs observed at 1733 cm^{-1} and 1243 cm^{-1} can be related to the reduction in hemicellulose. This phenomenon was explained by Yadav and Malanson [38] as follows. Starting from the 14th day, hemicelluloses is decomposed by microorganisms in the soil. Consequently, the lignin increases as is reflected by the sharp peak of the band at 1606 cm^{-1}. This is in line with Yadav and Malanson [38] who explained that because lignin is the most resistant fraction of the plant, it is the last fraction that decomposes in the soil.

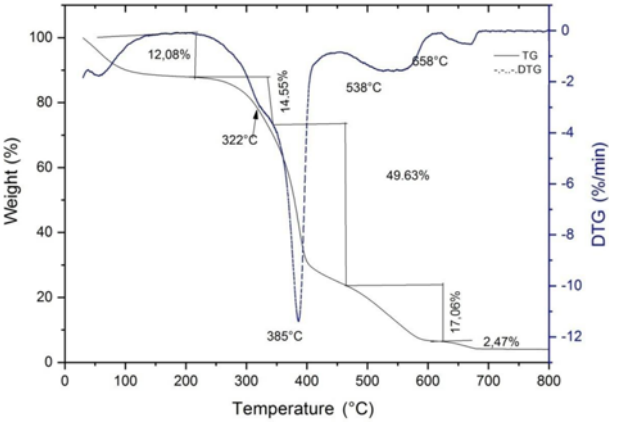

Figure 4. ATG/DTG of a BF.

In conclusion, the FTIR analysis of the BF extracted from *Agave americana L* leaves buried in soil confirms the existence of the major compounds like cellulose, hemicellulose, and lignin in their structure. In addition, this analysis correlated perfectly with the results of their chemical characterization.

X-ray Diffraction Analysis

Figure 4 shows the XRD spectrum of a BF. The presence of the four localized peaks 2θ=15, 16.4, 22.8 and 34.7 represents respectively the diffraction angle of the plane of the Miller indices (1-10), (110), (002) and (040) characteristic of the native cellulose I. In total agreement with Sari *et al.* [67], the peak, observed at 16.4 ^{o} can be attributed to the presence of non-cellulosic materials (e.g., hemicelluloses and lignin) in the BF. The peak at 2θ=22.8 ^{o} is attributed to crystallographic plane (002) which directs crystalline material (cellulose). The peak at 30.10 ^{o} attributed to an unknown contamination, probably from an inorganic substance [68,69]. The small peak at 34.5 ^{o} corresponds toa quarter of the length of one cellobiose unit and arises from ordering along the fiber direction. These observations confirm previous findings by Suryanto *et al.* [70]. In addition, these peaks correlate with peaks reported for *Agave americana* fibers extracted using distilled water and seawater [35]. But there are two types of native cellulose Iα and Iβ. The equation (3) $Z=1693d_1-902d_2-549$ by [34] was used to determine the type and crystal structure of cellulose. If $Z>0$ indicates that the triclinic structure (Iα) is found in bacterial cellulose and algae. In contrast, if $Z<0$ indicates a monoclinic structure Iβ, the negative Z value for BF (-33.2) indicates that the cellulose in these fibers is of the dominant type Iβ. Therefore, this finding corroborates with the FTIR, and XRD analyses to confirm the existence of cellulose type Iβ.

The next finding was related to the crystallinity index of the BF extracted from *Agave americana* after its leaf burial in the soil. This index was 53 %. In this, it differs with other extraction methods. Indeed, the index revealed in our work exceeded the 47.15 % crystallinity index of the fibers of the *Cissus quadrangularis* stem retted in water and reported by Indran and Raj [71]. Similarly, it was much higher than the 41.2 % and the 50.1 % indices revealed by El Oudiani *et al.* [35] after retting the *Agave americana* leaves in seawater and in distilled water, respectively. Similarly, other studies revealed lesser crystallinity indices for other fibers. For instance, *Lygeum spartum* fibers had 46.19 % and *Ferula communis* fibers had 48 % [65], *Wrightia tinctoria* fibers had 49.2 % [72] and fibers from *Date Palm* had only 19.9 % [63]. A higher crystalline index indicates well-oriented cellulose crystals along the axis of the fiber which would give the fiber more strength. Hence, it can be conclude that the extraction of the BF through burial of the leaves in the soil would enhance their strength. The crystalline size equation (2) was applied at the peak (002), the crystallite size (L) of BF from *Agave americana* (2.87 nm) is higher than that found in the *eucalyptus grandis* fiber 2.11, *Pinus elliottii* 1.92, *Dipteryx odorata* 2.18, *Mezilaurus itauba* 2.23, Kenaf 2.71 [73]. Abdal-hay *et al.* [74] discovered that crystallite size was directly related to the crystallinity index [75]. The greater the crystalline size, the higher the crystallinity index becomes. The increase in crystallinity is due to the decrease of the amorphous region. Furthermore, as was revealed by Suryanto *et al.* [70], the crystalline size of cellulose increases its thermal stability analyzed below.

Thermal Analysis

Lignocellulosic fiber components are cellulose, hemicellulose and lignin. These components decompose at different temperatures because of the difference in their chemical composition. Indeed, whereas hemicelluloses decomposes at temperatures ranging between 200 to 260 ^{o}C, cellulose decomposes at temperatures ranging between 240 to 350 ^{o}C and lignin decomposes at temperatures ranging between 280 to 500 ^{o}C.

Figure 4 presents the TG and DTG analysis of the BF. A weight loss of 12.08 % BF was observed atthe range of 30 to 103 ^{o}C due to the evaporation of the water in the fibers. In addition, the weight loss is attributed to the evaporation of the water and the other volatile extracts present in the BF [76]. Nagaraja-Ganesh and Muralikannan [77] explained this increased temperature of moisture loss by the high degree of hydrogen bonding between cellulose and water. This is due to the increase in the number of hydroxyl groups. Therefore, the hydrophilic behavior of BF and other fibers. Figure 4 shows two main peaks. The first appears at the range of 215 to 342 ^{o}C and is centered at 322 ^{o}C of the BF with 14.55 % of weight loss. It can be associated with the decomposition of hemicelluloses, pectin and the glycoside linkages of cellulose as was previously reported by Fiore *et al.* [78]. This finding corroborates with the FTIR study and confirms the presence of the glycosidic linkages. The second major peak observed at the range of 344 ^{o}C to 464 ^{o}C and centered at 385 ^{o}C of the BF can be is due to the decomposition of cellulose. Similar peaks to this one were observed in various natural fibers such as *okra* 359 ^{o}C [66] *Lygeum spartum L* 338 ^{o}C [79]. *Sansevieria ehrenbergii* 333.02 ^{o}C [80], curaua 344 ^{o}C, jute 365 ^{o}C, kenaf 364 ^{o}C, ramie 357 ^{o}C and sisal fibers 347 ^{o}C [74]. The sharpest peak intensity in BF is associated with high crystallinity of cellulose. Finally, the third small peak was observed at 538 ^{o}C of BF. It can be due to the decomposition of lignin. The need for a higher temperature for the degradation of lignin in the FB may be explained by the presence of polysaccharides and heavy cross linking of molecules [77]. Hence, this finding corroborates with the chemical and FTIR analyses above. The fourth peak at 658 ^{o}C can be associated with the decomposition of the molecules CO_2, CO, hydrocarbons

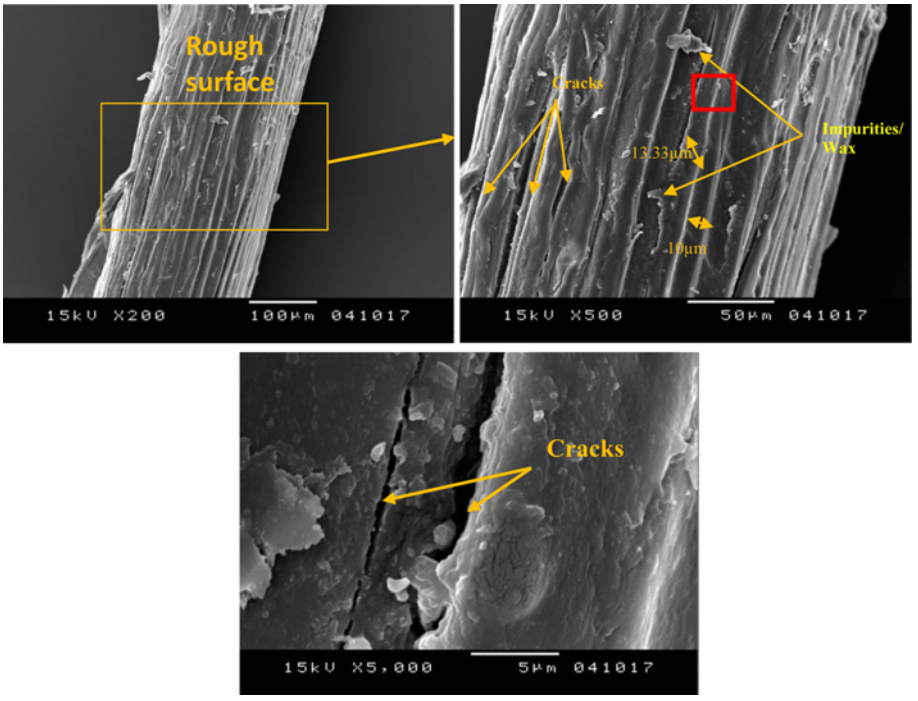

Figure 5. SEM of a BF.

and hydrogen as was reported by Indran and Raj [71].

Scanning Electron Microscope Analysis

Figure 5 show the result of the SEM. The BF contains a rough surface with cracks due to a bond break between microfibers. This surface contains a large number of fiber cells. These microfibers are characterized by diameters of about 10 to 15 µm as shown in Figure 5. In line with Oudiani *et al.* [35], the occurrence of such cracks can be attributable to the crystalline character of the fiber. Consequently, in line with Manimaran *et al.* [36], the surface roughness can be explained by an increase of adhesion in a fiber-polymeric matrix interface in the production of composites.

Conclusion

This study attempted to explore a new method of extracting BF from the *Agave americana L.* plant. After the burial of the plant leaves in the soil, the obtained fibers were submitted to a chemical, ATR-FTIR, XRD, SEM and Thermal analyses. The chemical analysis carried out on BF highlighted a high cellulose content (63 wt.%,) which offers higher strength on the fibers. The ATR-FTIR and X-ray analyses confirmed that BF is rich in cellulose, with a crystallinity index of 53 %. The thermo gravimetric analysis of BF revealed that it can thermally withstand a temperature of up to 215 °C. The SEM analysis showed that BF contains a large number of fiber cells aligned and a rough surface due to adhesion to matrix polymer. Through the obtained results it can be concluded that the burial in the soil approach would be an efficient and productive method of extraction of BF. It enhances the quality of the extracted fibers which would be a material of choice for reinforcement of polymer composites. They can have very useful applications in industry.

Acknowledgement

The authors would like to thank Dr Ayadi Hajji for his help with correcting, improving and editing the English of the manuscript.

References

1. N. A. Rosli, I. Ahmad, I. Abdullah, F. H. Anuar, and F. Mohamed, *Carbohydr. Polym.*, **125**, 69 (2015).
2. S. E. Hamdi, C. Delisée, J. Malvestio, N. Da Silva, A. Le Duc, and J. Beaugrand, *Compos. Part A Appl. Sci. Manuf.*, **76**, 1 (2015).
3. O. Faruk, A. K. Bledzki, H. P. Fink, and M. Sain, *Prog. Polym. Sci.*, **37**, 1552 (2012).
4. A. Hulle, P. Kadole, and P. Katkar, *Fibers*, **3**, 64 (2015).
5. S. Msahli, J. Ydrean, and F. Sakli, *Text. Res. J.*, **75**, 540 (2005).
6. T. Thamae and C. Baillie, *Compos. Interfaces*, **14**, 821 (2007).
7. P. Zakikhani, R. Zahari, M. T. H. Sultan, and D. L. Majid, *Mater. Des.*, **63**, 820 (2014).
8. F. D. A. Silva, B. Mobasher, C. Soranakom, and R. D. T.

Filho, *Cem. Concr. Compos.*, **33**, 814 (2011).
9. S. Ben Brahim and R. Ben Cheikh, *Compos. Sci. Technol.*, **67**, 140 (2007).
10. M. Jaouadi, S. Msahli, and F. Sakli, *Mater. Manuf. Process.*, **26**, 567 (2011).
11. M. A. Bouaziz, R. Rassaoui, and S. Besbes, *J. Chem.*, **2014**, Article ID 758697 (2014).
12. A. el Oudiani, Y. Chaabouni, S. Msahli, and F. Sakli, *Text. Res. J.*, **78**, 631 (2008).
13. A. Bessadok, S. Roudesli, S. Marais, N. Follain, and L. Lebrun, *Compos. Part A Appl. Sci. Manuf.*, **40**, 184 (2009).
14. K. Mylsamy and I. Rajendran, *Mater. Des.*, **32**, 4629 (2011).
15. A. El Oudiani, Y. Chaabouni, S. Msahli, and F. Sakli, *J. Text. Inst.*, **103**, 565 (2012).
16. D. E. Akin, *ISRN Biotechnol.*, **2013**, 23 (2013).
17. G. Henriksson, D. E. Akin, R. T. Hanlin, C. Rodriguez, D. D. Archibald, L. L. Rigsby, and K. L. Eriksson, *Appl. Environ. Microbiol.*, **63**, 3950 (1997).
18. D. E. Akin, B. Condon, M. Sohn, J. A. Foulk, R. B. Dodd, and L. L. Rigsby, *Ind. Crops Prod.*, **25**, 136 (2007).
19. A. Bezazi, A. Belaadi, M. Bourchak, F. Scarpa, and K. Boba, *Compos. Part B Eng.*, **66**, 194 (2014).
20. E. G. Jobbágy and R. B. Jackson, *Ecol. Appl.*, **10**, 423 (2000).
21. D. Mohamed, Ph.D. Dissertation, UHAM, Mulhouse, 2012.
22. R. G. Burns, J. L. DeForest, J. Marxsen, R. L. Sinsabaugh, M. E. Stromberger, M. D. Wallenstein, and A. Zoppini, *Soil Biol. Biochem.*, **58**, 216 (2013).
23. ASTM D1107-96, "Standard Test Method for Ethanol-toluene Solubility of Wood", ASTM International, West Conshohocken, PA, 2007.
24. ASTM D1110-84, "Standard Test Methods for Water Solubility of Wood", ASTM International, West Conshohocken, PA, 2013.
25. ASTM D1106-96, "Standard Test Method for Acid-insoluble Lignin in Wood", ASTM International, West Conshohocken, PA, 2013.
26. ASTM D1104-56, "Standard Test Method for Holocellulose in Wood", ASTM International, West Conshohocken, PA, 1978.
27. ASTM D1103-60, "Standard Test Method for Alpha-cellulose in Wood", ASTM International, West Conshohocken, PA, 1977.
28. ASTM D1102-84, "Standard Test Method for Ash in Wood", ASTM International, West Conshohocken, PA, 2013a.
29. A. Yadav and V. K. Garg, *J. Hazard. Mater.*, **168**, 262 (2009).
30. R. B. Bradstreet, *Analy Chem.,* **26**, 185 (1954).
31. W. Aldous and B. I. Armstrong, *Soil Sci.,* **37**, 29 (1934).
32. G. Pan, P. Smith, and W. Pan, *Agric. Ecosyst. Environ.*, **129**, 344 (2009).
33. L. Segal, J. J. Creely, A. E. Martin, and C. M. Conrad, *Text. Res. J.*, **29**, 786 (1959).
34. M. Wada and T. Okano, *Cellulose*, **8**, 183 (2001).
35. A. El Oudiani, Y. Chaabouni, S. Msahli, and F. Sakli, *J. Text. Inst.*, **100**, 430 (2009).
36. P. Manimaran, P. Senthamaraikannan, M. R. Sanjay, M. K. Marichelvam, and M. Jawaid, *Carbohydr. Polym.*, **181**, 650 (2018).
37. A. El Oudiani, R. Ben Sghaier, Y. Chaabouni, S. Msahli, and F. Sakli, *J. Text. Inst*., **103**, 349 (2012).
38. V. Yadav and G. Malanson, *Prog. Phys. Geogr.*, **31**, 131 (2007).
39. R. Kumar, N. R. J. Hynes, P. Senthamaraikannan, S. Saravanakumar, and M. R. Sanjay, *J. Nat. Fib.*, **15**, 822 (2018).
40. S. Indran, R. E. Raj, and V. S. Sreenivasan, *Carbohydr. Polym.*, **110**, 423 (2014).
41. I. I. Mukhtar, Z. Leman, E. S. Zainudin, and M. R. Ishak, *J. Nat. Fib.*, **15**, 1 (2018).
42. R. López-Mondéjar, D. Zühlke, D. Becher, K. Riedel, and P. Baldrian, *Sci. Rep.*, **6**, 25279 (2016).
43. S. S. Saravanakumar, A. Kumaravel, T. Nagarajan, P. Sudhakar, and R. Baskaran, *Carbohydr. Polym.*, **92**, 1928 (2013).
44. Q. Yang and X. Pan, *Bioresour. Technol.*, **126**, 336 (2012).
45. S. Hanana, A. Elloumi, V. Placet, H. Tounsi, H. Belghith, and C. Bradai, *Ind. Crop. Prod.*, **70**, 190 (2015).
46. M. Haddar, A. Elloumi, A. Koubaa, C. Bradai, and S. Migneault, *Ind. Crop. Prod.*, **121**, 26 (2018).
47. Taimur-Al-Mobarak, M. F. Mina, M. A. Gafur, A. N. Ahmed, and S. A. Dhar, *Fiber. Polym.*, **19**, 31 (2018).
48. J. Jayaramudu, A. Maity, E. R. Sadiku, B. R. Guduri, A. V. Rajulu, C. V. Ramana, and R. Li, *Carbohydr. Polym.*, **86**, 1623 (2011).
49. M. Mushtaq, H. Kasur, R. A. Khan, A. Khalid, and K. Iqbal, *J. Scienti. Res.,* **10**, 51 (2018).
50. H. A. Khalil, M. S. Hossain, E. Rosamah, N. A. Azli, N. Saddon, Y. Davoudpoura, and R. Dungani, *Renew. Sustain. Energy Rev.*, **43**, 1006 (2015).
51. I. Kögel-Knabner, *Soil Biol. Biochem.*, **105**, 3 (2017).
52. Y. Kuzyakov and G. Domanski, *J. Plant Nutr. Soil Sci.*, **163**, 421 (2000).
53. E. A. Paul, *Soil Biol. Biochem.*, **98**, 109 (2016).
54. A. K. Halder and P. K. Chakrabartty, *Folia Microb*., **38**, 325 (1993).
55. M. Ledin, C. Krantz-Rülcker, and B. Allard, *Soil Biol. Biochem.*, **31**, 1639 (1999).
56. M. Sadowsky and M. Schortemeyer, *Global Change Biology*, **3**, 217 (1997).
57. T. P. Sathishkumar, P. Navaneethakrishnan, S. Shankar, and R. Rajasekar, *Compos. Interfaces*, **20**, 575 (2013).
58. S. S. Saravanakumar, A. Kumaravel, T. Nagarajan, and I. G. Moorthy, *Int. J. Poly. Anal. Character.*, **19**, 309 (2014).
59. P. Ganeshan, B. Nagaraja Ganesh, P. Ramshankar, and K. Raja, *Int. J. Poly. Anal. Character*., **23**, 271 (2018).

60. P. Senthamaraikannan and M. Kathiresan, *Carbohydr. Polym.*, **186**, 332 (2018).
61. K. O. Reddy, C. U. Maheswari, M. S. Dhlamini, B. M. Mothudi, V. P. Kommula, J. Zhang, and A. V. Rajulu, *Carbohydr. Polym.*, **188**, 85 (2018).
62. A. Porras, A. Maranon, and I. A. Ashcroft, *Compos. Part B Eng.*, **74**, 66 (2015).
63. S. C. Pereira, L. Maehara, C. M. M. Machado, and C. S. Farinas, *Renew. Energy*, **87**, 607 (2016).
64. K. O. Reddy, B. Ashok, K. R. N. Reddy, Y. E. Feng, J. Zhang, and A. V. Rajulu, *Int. J. Polym. Anal. Charact.*, **19**, 48 (2014).
65. Y. Seki, M. Sarikanat, K. Sever, and C. Durmuşkahya, *Compos. Part B Eng.*, **44**, 517 (2013).
66. I. M. De Rosa, J. M. Kenny, M. Maniruzzaman, M. Moniruzzaman, M. Monti, D. Puglia, and F. Sarasini, *Compos. Sci. Technol.*, **71**, 246 (2011).
67. N. Herlina Sari, I. N. G. Wardana, Y. S. Irawan, and E. Siswanto, *J. Nat. Fiber*, **15**, 545 (2018).
68. A. L. S. Pereira, D. M. do Nascimento, M. S. Men de Sá Filho, A. R. Cassales, J. P. Morais, R. C. Paula, M. F. Rosa, and J. P. Feitosa, *BioResources*, **9**, 7749 (2014).
69. C. Chen, W. Yin, G. Chen, G. Sun, and G. Wang, *J. Mater.,* **10**, 514 (2017).
70. H. Suryanto, A. A. Fikri, A. A. Permanasari, U. Yanuhar, and S. Sukardi, *J. Nat. Fiber*, **15**, 406 (2018).
71. S. Indran and R. E. Raj, *Carbohydr. Polym.*, **117**, 392 (2015).
72. K. Subramanian, P. Senthil Kumar, P. Jeyapal, and N. Venkatesh, *Eur. Polym. J.*, **41**, 853 (2005).
73. M. Poletto, H. L. Ornaghi Júnior, and A. J. Zattera, *Materials (Basel)*, **7**, 6105 (2014).
74. A. Abdal-hay, N. P. G. Suardana, D. Y. Jung, K.-S. Choi, and J. K. Lim, *Int. J. Precis. Eng. Manuf.*, **13**, 1199 (2012).
75. U. J. Kim, S. H. Eom, and M. Wada, *Polym. Degrad. Stab.*, **95**, 778 (2010).
76. P. Ganeshan, B. Nagaraja Ganesh, P. Ramshankar, and K. Raja, *Int. J. Poly. Anal. Character.,* **23**, 271 (2018).
77. B. Nagaraja Ganesh and R. Muralikannan, *Int. J. Poly. Anal. Character*, **21**, 244 (2016).
78. V. Fiore, T. Scalici, and A. Valenza, *Carbohydr. Polym.*, **106**, 77 (2014).
79. Z. Belouadah, A. Ati, and M. Rokbi, *Carbohydr. Polym.*, **134**, 429 (2015).
80. T. P. Sathishkumar, P. Navaneethakrishnan, S. Shankar, R. Rajasekar, and N. Rajini, *J. Reinf. Plast. Compos.*, **32**, 1457 (2013).